

# Computer simulation studies of aqueous sodium chloride solutions at 298 K and 683 K

S. Koneshan<sup>a)</sup> and Jayendran C. Rasaiah<sup>b)</sup>

*Department of Chemistry, University of Maine, Orono, Maine 04469*

(Received 3 May 2000; accepted 10 August 2000)

We have carried out molecular dynamics simulations of NaCl solutions at room temperature (298 K) and at a supercritical temperature of 683 K using discrete simple point charge (SPC or SPC/E) molecular models for the water solvent. The solvent densities were  $0.997 \text{ g cm}^{-3}$  at 298 K and  $0.35 \text{ g cm}^{-3}$  and  $0.175 \text{ g cm}^{-3}$  at 683 K. The ion-ion and ion-solvent distribution functions were calculated and compared with corresponding functions for a continuum model of the solvent also determined by computer simulation. Our studies confirm the presence of significant amounts of ion pairing and clustering at supercritical conditions as seen in visualizations of the equilibrium configurations of the solution. However, the degree of pairing and clustering of ions in supercritical solutions is significantly different for discrete and continuum representations of the solvent. Simulations of a 1 molal solution of NaCl at 683 K, using a discrete molecular model for the solvent at a density of  $0.35 \text{ g cm}^{-3}$ , show the presence of a single megacluster of 10 sodium and chloride ions in a system of 555 water molecules. Three smaller clusters containing positive and negative charges are observed at 683 K when the electrolyte concentration is reduced to 0.5 molal at a solvent density of  $0.35 \text{ g cm}^{-3}$  and also at a lower solvent density of  $0.175 \text{ g cm}^{-3}$ . Molecular dynamics simulations of the velocity auto correlation functions of  $\text{Na}^+$  and  $\text{Cl}^-$  ions have distinct forms related to the cluster to which the ion belongs. The diffusion coefficients of  $\text{Na}^+$  and  $\text{Cl}^-$  ions, at infinite dilution, are larger at 683 K than at 298 K, and decrease with increasing electrolyte concentration. They are nearly equal to each other in the one molal solution at 683 K, which may correspond to a supersaturated solution in which the large cluster of sodium and chloride ions moves as an entity over an observed lifetime greater than 200 ps. © 2000 American Institute of Physics. [S0021-9606(00)50242-6]

## I. INTRODUCTION

The dielectric properties of water influence the dissociation of an electrolyte and subsequent solvation of ions in aqueous solutions. Oppositely charged ions in aqueous solutions tend to associate when the temperature is increased, which is evident from the conductivity measurements of aqueous electrolyte solutions carried out at supercritical temperatures by Quist and Marshall<sup>1</sup> and by Wood *et al.*<sup>2</sup> This phenomenon is explained qualitatively by the observed decrease in the dielectric constant of water from nearly 78 at ambient temperatures to approximately 5 near critical conditions. The dielectric properties of water also change with the solvent density, and correlations of the experimental dielectric constant with temperature and density were discussed recently by Fernandez *et al.*<sup>3</sup>

The decrease in the dielectric constant with temperature is also observed in computer simulation studies of simple point charge models (SPC and SPC/E) for water. Mountain and Wallquist,<sup>4</sup> Cui and Harris,<sup>5</sup> Neumann,<sup>6</sup> and Guissani and Guillot<sup>7</sup> have published details of their simulations of the dielectric constant of water over wide ranges of temperature and density. These simulations, using the SPC or SPC/E models for water, are generally in agreement with the experi-

mental dielectric constant and transport properties of water, such as the diffusion coefficient. This gives us confidence in employing the same models to study the properties of ionic solutions at elevated temperatures by computer simulation.

Supercritical water is characterized by a large compressibility  $\kappa_T$  that is related to density fluctuations in an open system and the solvent pair correlation function  $g(r)$  through the well-known compressibility equation<sup>8</sup>

$$\rho_w k T \kappa_T = 1 - \rho_w \int (g(r) - 1) dr. \quad (1)$$

Here  $\rho_w$  is the number density of water,  $k$  is Boltzmann's constant,  $T$  is the temperature in degrees Kelvin, and the integration is over all space. The high compressibility in the critical region allows for large variations in the solvent density with small changes in the external pressure. The effect of solvent density fluctuations on ion solvation, association, and ionic reactions at supercritical temperatures however, is less well understood, and is currently an active area of research.<sup>9,10</sup>

Computer simulations of the potential of mean force of NaCl (Chiavio and Cummings,<sup>11</sup> Dang *et al.*,<sup>12</sup> Rey and Guardia *et al.*,<sup>13</sup> Berkowitz *et al.* and Karim *et al.*<sup>14</sup>) in solution at ambient conditions suggest that association of  $\text{Na}^+$  and  $\text{Cl}^-$  ions takes place in two or more steps. In its simplest form, this is represented schematically as<sup>11</sup>



<sup>a)</sup>Current address: Department of Computer Science, Cornell University, Ithaca, New York.

<sup>b)</sup>Author to whom correspondence should be addressed.

Here  $\text{Na}^+|\text{Cl}^-$  represents a solvent separated ion pair, and  $\text{Na}^+\text{Cl}^-$  is a contact ion pair. This scenario underscores the intimate role that the solvent plays, beyond its dielectric properties, in the association of oppositely charged ions to form pairs. However the interionic distance between sodium and chloride ions is a poor reaction coordinate since the transmission coefficient is low<sup>14</sup> and Geissler *et al.*<sup>15</sup> have discussed how solvent fluctuations and collective motions determine kinetic pathways for this reaction.

The effect of ions on the properties of a polar solvent like water near its critical region is also of great theoretical and experimental interest.<sup>16–19</sup> They could conceivably shift the critical constants and alter the critical exponents of the solvent. Conversely the solvent, which mediates the interactions between ions through its dielectric properties and charge screening, could promote the formation of clusters of positive and negative ions with intervening solvent molecules. This may even lead to charge density waves, as discussed by Nabutovskii *et al.*<sup>20</sup> and Høye and Stell.<sup>21</sup>

In this paper, we describe molecular dynamics simulations of NaCl solutions at 298 and 683 K, using discrete and continuum models for the solvent. We first present our results for 1.0 and 0.5 molal NaCl solutions using discrete models for the solvent. The study at 298 K is at the usual solvent density of 0.997 g cm<sup>-3</sup>, while the simulations of the one molal sodium chloride at 683 K were carried out at a solvent density of 0.35 g cm<sup>-3</sup> which is close to the critical density of water which is 0.32 g cm<sup>-3</sup>. Our studies are nearly 30° above the critical temperature of water. The high temperature (683 K) studies of the 0.5 molal NaCl solution were performed at two different solvent densities of 0.35 and 0.175 g cm<sup>-3</sup> to investigate the effect of this variable on the properties of the system under supercritical conditions. Sodium chloride is sparingly soluble in water at high temperatures, and the one molal solution of NaCl in SPC water at 683 K discussed in our studies may correspond to a supersaturated solution, while the 0.5 molal solutions should represent concentrated salt solutions at 683 K. We also present results of molecular dynamics studies of one molal sodium chloride solutions at 298 K and at 683 K using a continuum model for the solvent with appropriate dielectric constants of 78 and 5, respectively. This allows us to compare the properties of an electrolyte at the same concentration in solutions that differ primarily in the treatment of the solvent as a continuum dielectric medium or discrete molecular medium.

We determine the pair correlation functions and diffusion coefficients of the ions in NaCl solutions at 298 K and 683 K and compare them with each other and with the corresponding data at infinite dilution.<sup>22,23</sup> This enables us to characterize the essential features that distinguish electrolyte solutions at supercritical temperatures from the same solutions at ambient temperature. The main difference observed in our simulations between the 1 molal and 0.5 molal sodium chloride at high and low temperatures, is the clustering of the sodium and chloride ions in supercritical region of the solvent that goes beyond the formation of isolated ion pairs. The formation of small clusters of ions eventually organizing into a larger mass with increasing temperature was also observed previously by Driesner *et al.*<sup>24</sup> and Tester *et al.*<sup>25,26</sup> in

TABLE I.  $\text{Na}^+$ -water,  $\text{Cl}^-$ -water, ion-ion, and water-water potential parameters.

Ion	$\sigma_{io}$ (Å)	$\epsilon_{io}$ (kJ/mol)	$\sigma_{ih}$ (Å)	$\epsilon_{ih}$ (kJ/mol)
$\text{Na}^+$	2.72	0.560 14	1.310	0.560 14
$\text{Cl}^-$	3.55	1.505 75	2.140	1.505 75
Ion pair	$\sigma$ (Å)	$\epsilon$ (kJ/mol)		
$\text{Na}^+\text{Na}^+$	2.443	0.119 13		
$\text{Na}^+\text{Cl}^-$	2.796	0.352 6		
$\text{Cl}^-\text{Cl}^-$	3.487	0.979 06		
Water	$\sigma_{oo}$ (Å)	$\epsilon_{oo}$ (kJ/mol)	Charge ( <i>q</i> )	
O(H <sub>2</sub> O)	3.156	0.650 20	-0.82	
H(H <sub>2</sub> O)			+0.41	

their simulations of NaCl solutions in supercritical water. Our study investigates the diffusion of the ions and ion clusters at supercritical temperatures as well as the diffusion of free ions at room temperature.

We find that the diffusion coefficients of the sodium and chloride ions at infinite dilution determined in the discrete solvent models for water increase sharply with rise in temperature. This is similar to the behavior of other simple cations and anions, reported by us in recent studies,<sup>22,23</sup> and agrees with the trends shown by experimental determinations of the mobilities of ions in water at infinite dilution.<sup>1,2</sup> We also find that the ion diffusion coefficients decrease with increasing salt concentration, as expected from theory. The decrease is much greater for supercritical solutions than it is for solutions under ambient conditions. At a sufficiently high salt concentration, the clusters of sodium and chloride ions diffuse as single entities and the ionic diffusion coefficients of the  $\text{Na}^+$  and  $\text{Cl}^-$  ions become essentially equal to each other.

We also discuss simulations of sodium chloride solutions using a continuum model for the solvent. Although, the qualitative features of the structure and dynamics of sodium and chloride solutions using a continuum and discrete solvent models remain the same in our simulations of 1 molal NaCl solutions, there are important differences in the details. For example, the extent of pairing and clustering of ions observed at 683 K in the continuum and discrete representations of the solvent are significantly different. This shows that dielectric continuum models, while useful in many respects, are oversimplified caricatures of real electrolyte solutions at supercritical temperatures due to solvent inhomogeneity caused by density fluctuations.

There have been other investigations of aqueous solutions of NaCl at ambient and supercritical temperatures, apart from the studies of Driesner *et al.*,<sup>24</sup> Tester, Harris, and their groups,<sup>25,26</sup> and Chiavlo and Cummings.<sup>11</sup> Hummer *et al.*<sup>27</sup> studied the equilibrium properties of aqueous solutions of NaCl at several concentrations and at temperatures ranging from ambient to supercritical conditions, by simulation and calculation of the ion correlation functions using integral equation approximations. These studies have a different perspective from ours, which investigates the diffusion

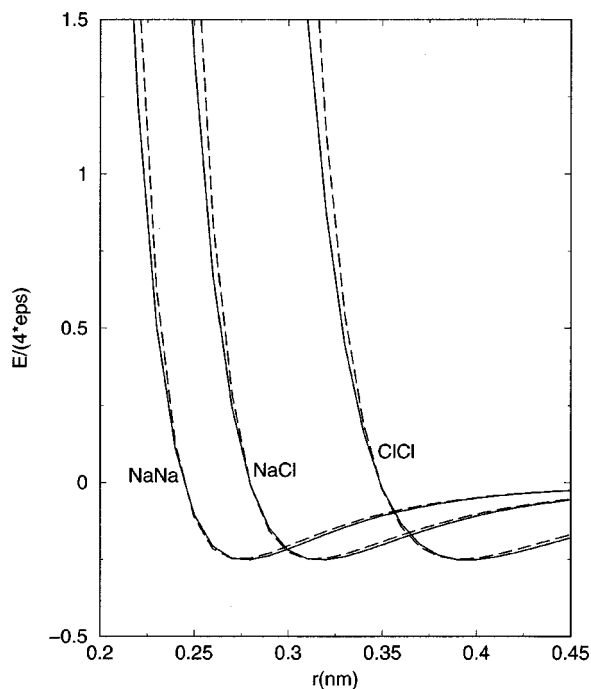


FIG. 1. Comparison of the non-Coulombic interactions between  $\text{Na}^+$  and  $\text{Cl}^-$  ions using Huggins–Mayer (solid line) and Lennard-Jones (dashed line) potentials. The Lennard-Jones parameters  $\epsilon$  and  $\sigma$  were calculated from the Huggins–Mayer potential and Eq. (8). Both models give potential functions that coincide closely in the regions shown.

of ions in solution and their relation to cluster formation at high temperature.

## II. MOLECULAR DYNAMICS SIMULATION TECHNIQUES

Our primary system of ions in a discrete aqueous solvent consisted of 10  $\text{Na}^+$ , 10  $\text{Cl}^-$ , and 555 SPC water molecules. This represents a NaCl solution at a 1 molal concentration of electrolyte. The density of water in our simulations was  $0.997 \text{ g cm}^{-3}$  at 298 K and  $0.35 \text{ g cm}^{-3}$  at 683 K. These values of the solvent density require cubic simulation cell box lengths of  $25.54 \text{ \AA}$  and  $36.20 \text{ \AA}$ , respectively. The number of water molecules was increased by a factor of 2 for the simulations of 0.5 molal NaCl solutions carried out at solvent densities of  $0.35 \text{ g cm}^{-3}$  and  $0.175 \text{ g cm}^{-3}$  at 683 K; they correspond, in our simulations, to cubic box lengths of  $45.6 \text{ \AA}$  and  $57.5 \text{ \AA}$ , respectively. The correlation length is given by<sup>25</sup>

$$\xi = \xi_0 (\Delta T)^{-\nu} [1 + \xi_1 (\Delta T)^{\Delta_1} + \dots], \quad (2)$$

where  $\Delta T = (T - T_c)/T_c$ ,  $\nu = 0.63$ , and  $\Delta_1 = 0.51$ . For water  $\xi_0 = 1.3$  and  $\xi_1 = 2.16$ . At 683 K the correlation length is  $11 \text{ \AA}$ , which is considerably smaller than half the box length in all cases considered.<sup>28</sup>

The parameters  $\sigma_{oo}$  and  $\epsilon_{oo}$  for the interactions between water molecules displayed in Table I are for the simple point charge (SPC) for water with the potential energy of interaction between two water molecules given by

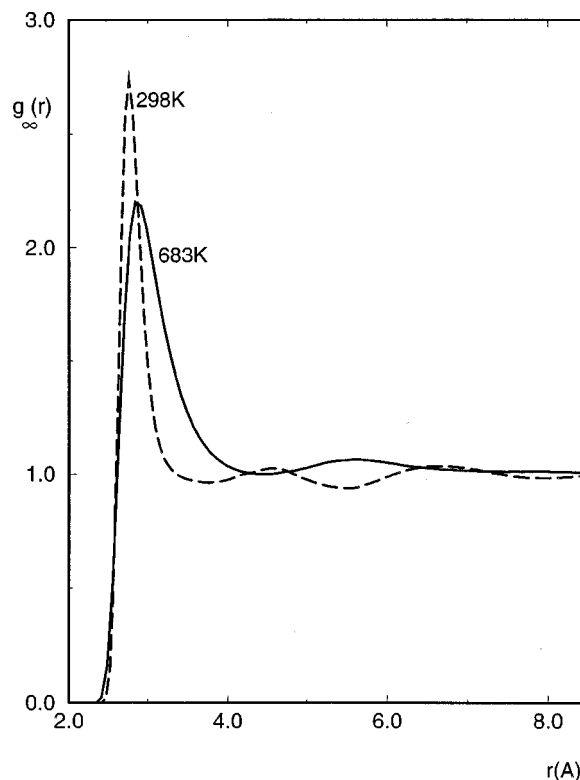


FIG. 2. Oxygen–oxygen radial distribution function at 298 K ( $0.997 \text{ g cm}^{-3}$  of SPC water, dashed line) and 683 K ( $0.35 \text{ g cm}^{-3}$  of SPC water, solid line) in a 1 molal NaCl solution.

$$u_{\text{water}} = 4\epsilon_{oo} \left[ \left( \frac{\sigma_{oo}}{r_{oo}} \right)^{12} - \left( \frac{\sigma_{oo}}{r_{oo}} \right)^6 \right] + \frac{1}{4\pi\epsilon_0} \sum_{i=1}^3 \sum_{j=1}^3 \frac{q_i q_j}{r_{ij}}. \quad (3)$$

Here  $\epsilon_0$  is the permittivity of free space. The ion–water and ion–ion potentials consist of Lennard-Jones and Coulombic components. The Lennard-Jones (LJ) interaction between two water molecules is only between the oxygen atoms, and the corresponding LJ ion–water interactions are between the ion–oxygen and ion–hydrogen atoms of SPC water. They are both of the form

$$u(r) = 4\epsilon \left[ \left( \frac{\sigma}{r} \right)^{12} - \left( \frac{\sigma}{r} \right)^6 \right], \quad (4)$$

with subscripts ( $i$ ,  $o$ , and  $h$ ) for  $\epsilon$  and  $\sigma$  to distinguish between the different water–water and ion–water LJ potentials as displayed in Table I.

The  $\epsilon$  and  $\sigma$  parameters for the ion–water and ion–ion LJ potentials were chosen to match the Pettit–Rossky<sup>29</sup> parameters for the Huggins–Mayer<sup>30</sup> potential for the non-Coulombic part of the interaction

$$u(r) = A \exp(-Br) - \frac{C}{r^6}. \quad (5)$$

Taking  $C = 4\epsilon\sigma^6$  and  $A = 4\epsilon \exp(B\sigma)$ , we have

$$u(r) = 4\epsilon \left[ \exp B(\sigma - r) - \left( \frac{\sigma}{r} \right)^6 \right]. \quad (6)$$

TABLE II. Coordination numbers in the primary shells of water and ions.

	298 K		683 K	
	1 molal <sup>a</sup>	1 molal <sup>b</sup>	0.5 molal <sup>b</sup>	∞ diln <sup>a</sup>
H <sub>2</sub> O	4.6	4.1	4.1	4.3
Na <sup>+</sup>	5.4	0.8	1.5	5.8
Cl <sup>-</sup>	8.0	5.2	7.2	7.2

<sup>a</sup>Solvent density 0.997 g cm<sup>-3</sup>.<sup>b</sup>Solvent density 0.35 g cm<sup>-3</sup>.

This implies that  $u(r)=0$  at  $r=\sigma$ . Requiring also that  $u(r)=-\epsilon$  at  $r=2^{1/6}\sigma$ , fixes the value of  $B\sigma$  through the relation

$$B\sigma = \left( \frac{1}{1-2^{1/6}} \right) \ln \left( \frac{1}{4} \right) = 11.36. \quad (7)$$

It follows that  $A=4\epsilon \exp(11.36)$  and the L-J parameters  $\epsilon$  and  $\sigma$  are related to parameters  $A$  and  $C$  of the Huggins-Mayer potential through the relations

$$\epsilon = \left( \frac{A}{4} \right) \exp(-11.36) = 2.91 \times 10^{-6} A, \quad (8)$$

$$\sigma = \left[ \left( \frac{C}{A} \right) \exp(11.36) \right]^{1/6} = 6.6414 \left( \frac{C}{A} \right)^{1/6}.$$

Figure 1 compares the Huggins-Mayer and Lennard-Jones potentials for the non-Coulombic interaction between Na<sup>+</sup> and Cl<sup>-</sup>. The Lennard-Jones potential is seen to be essentially identical to the Huggins-Mayer form except

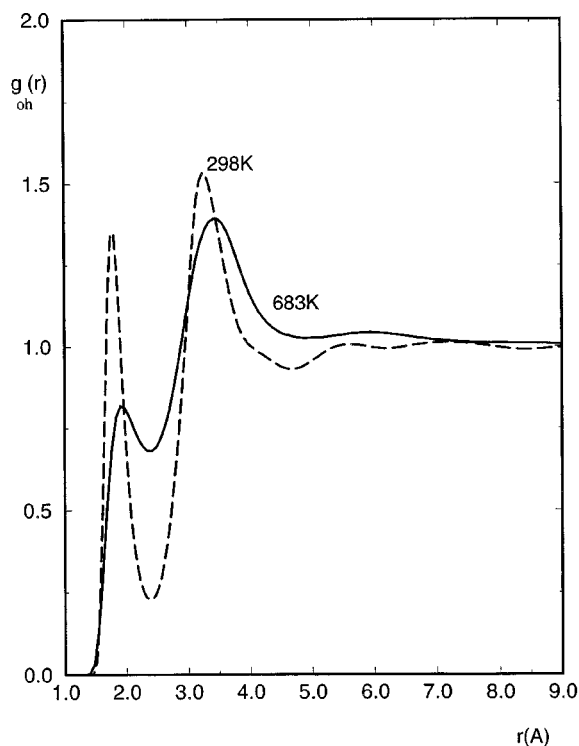


FIG. 3. Oxygen-hydrogen radial distribution function at 298 K (0.997 g cm<sup>-3</sup>, dashed line) and 683 K (0.35 g cm<sup>-3</sup>, solid line) in a 1 molal NaCl solution in SPC water. The hydrogen bonding peak height at 2.1 Å decreases as the temperature rises from 298 K to 683 K, signifying less hydrogen bonding at elevated temperatures.

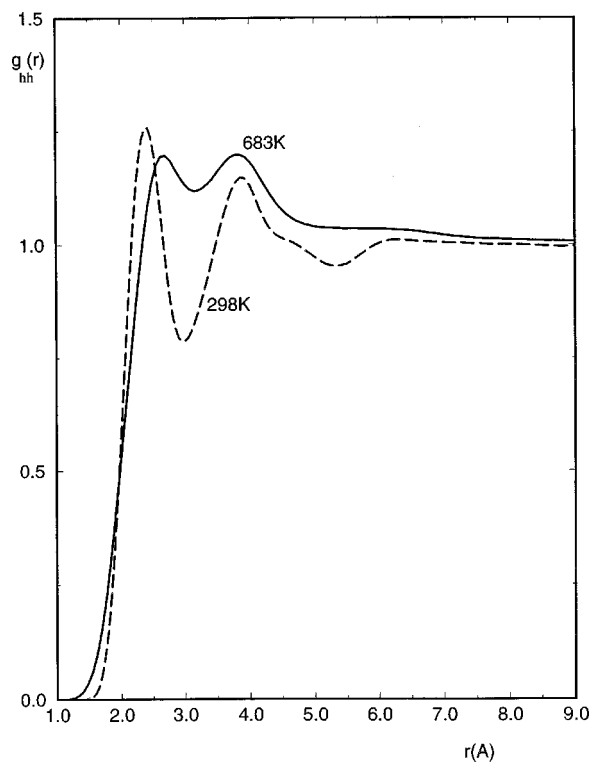


FIG. 4. Hydrogen-hydrogen radial distribution function at 298 K (0.997 g cm<sup>-3</sup>, dashed line) and 683 K (0.35 g cm<sup>-3</sup>, solid line) in a 1 molal NaCl solution in SPC water. Note the broadening and overlapping of the two peaks at elevated temperatures accompanying the decrease in hydrogen bonding.

when  $r \rightarrow 0$  when the latter is unphysical as  $u(r) \rightarrow -\infty$ . This observation and computational convenience dictated our preference for the Lennard-Jones form for the non-Coulombic interactions between ions and between ion and water in our simulations.

The NVT ensemble molecular dynamics simulations were carried out using a quaternion formulation for water available with the DLPOLY suite of programs (Daresbury Laboratory, United Kingdom) and was checked against our own programs using the same method. The time step was 1 fs, and the equilibration was over a period of nearly 1 ns. Production runs were examined over periods of 250 ps. Periodic boundary conditions were used in our calculations and the electrostatic interactions were determined by Ewald summation.

The results for Na<sup>+</sup> and Cl<sup>-</sup> ions in SPC/E water at infinite dilution and 683 K are taken from a collateral study<sup>22,23</sup> of our group. The SPC/E model is a modification of the SPC model that takes account of the polarizability of the water in an approximate way. The ion-water parameters for the model are tabulated in Ref. 22 and are taken from studies by Dang and his group<sup>31</sup> in which the  $\epsilon$  and  $\sigma$  for the ion-water interactions are fitted to the heats of hydration of small ion-water clusters. The difference between the two models, SPC and SPC/E, for water is negligible in comparisons of the qualitative features of the structure and mobilities of ions in solution.

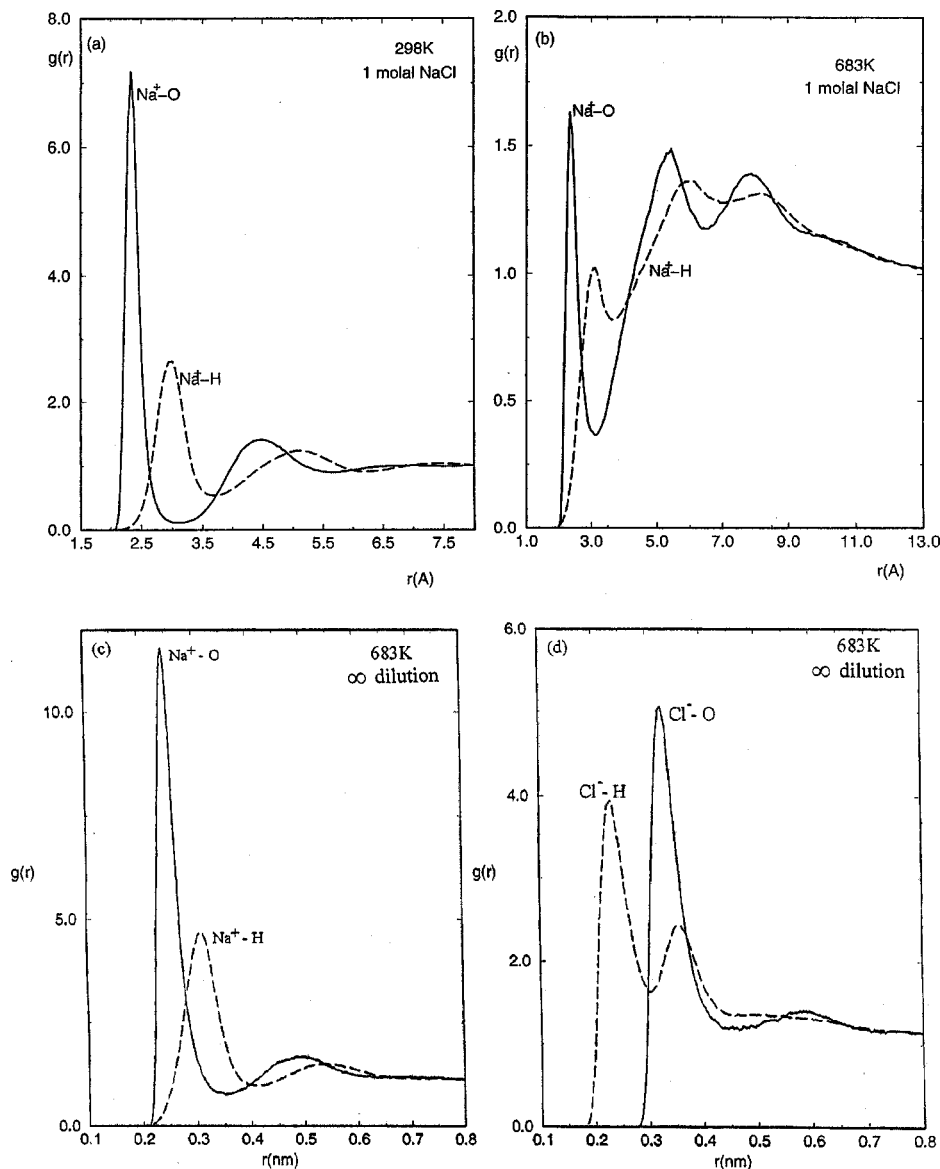


FIG. 5. (a) Sodium–oxygen (solid line) and sodium–hydrogen (dashed line) radial distribution functions at 298 K ( $0.997 \text{ g cm}^{-3}$ ) and 683 K ( $0.35 \text{ g cm}^{-3}$ ) in a 1 molal NaCl solution in SPC water. At 298 K, the distribution functions are in close agreement with those for a single sodium ion at infinite dilution. At 683 K, (b) shows three distinct sodium–oxygen peaks. Each of the peaks correlates with a corresponding sodium–hydrogen peak shown in the same figure. For comparison, (c) and (d) show the ion–oxygen (solid line) and ion–hydrogen (dashed line) radial distribution functions at 683 K for sodium and chloride ions in an infinitely dilute solution at a solvent density of  $0.35 \text{ g cm}^{-3}$ .

### III. RESULTS

We present our results for the equilibrium correlation functions before discussing the diffusion coefficients of  $\text{Na}^+$  and  $\text{Cl}^-$  ions at infinite dilution in SPC/E water at 298 K and in 0.5 and 1 molal sodium chloride solutions in SPC water at 683 K. While the properties of SPC and SPC/E water are similar to that of real water at ambient and supercritical temperatures, they are still only models representing water as a fluid or solvent. However, we believe they capture the essential physics of the interactions in these solutions, and our simulations of these model systems could be considered as a guide to the behavior of real ionic solutions in the supercritical region and at room temperature. We then discuss our simulations of one molal sodium chloride solutions at 298 K and 683 K using a continuum model for the solvent with dielectric constants of 78 and 5, respectively.

#### A. Solvent atom distribution functions

We determined the oxygen–oxygen, oxygen–hydrogen, and hydrogen–hydrogen radial distribution functions of wa-

ter in the neat solvent and in NaCl solutions in the usual way from histograms. Figure 2 shows the oxygen–oxygen radial distribution function  $g_{oo}(r)$  at 298 K ( $0.997 \text{ g/cm}^3$ , dashed line) and 683 K ( $0.35 \text{ g/cm}^3$ , solid line) for SPC water in 1 molal NaCl. It shows three peaks at room temperature corresponding to first, second, and third nearest neighbors. The third peak, which lies furthest away from the central oxygen atom, disappears at elevated temperatures while the first two peaks are shifted away from the origin at high temperatures as shown in Fig. 2. The hydration numbers in the first shell, were calculated from the integral

$$N_h = \rho_w \int_0^{R_U} g_{oo}(r) 4\pi r^2 dr. \quad (9)$$

Here  $R_U$  is the outer radius of the hydration shell and  $\rho_w$  is the number density of water. The results are summarized in Table II.

The locations of the first and second peaks of the  $g_{oo}(r)$  in NaCl solutions are similar to the corresponding peaks for pure water, but the peak heights are slightly different. The



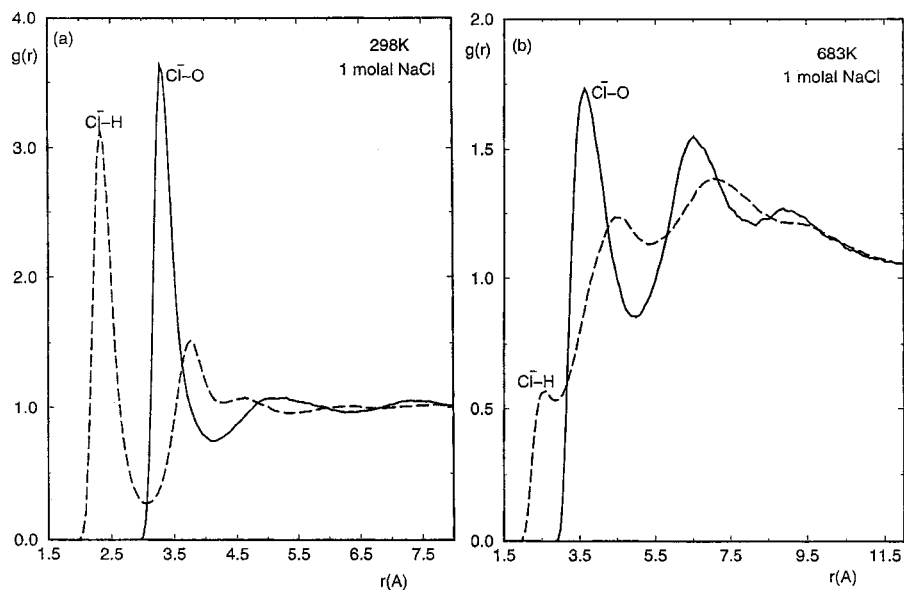


FIG. 6. Chloride–oxygen (solid line) and chloride–hydrogen (dashed line) radial distribution functions at 298 K (0.997 g cm<sup>-3</sup>) and 683 K (0.35 g cm<sup>-3</sup>) in a 1 molal NaCl solution in SPC water. At 298 K, the distribution functions are in close agreement with the corresponding functions for a single chloride ion at infinite dilution. At 683 K, (b) shows three different chloride–oxygen peaks. Each peak correlates with a corresponding chloride–hydrogen peak shown in the same figure. At 683 K Na<sup>+</sup> and Cl<sup>-</sup> ions are close to each other in a cluster.

coordination number of SPC water at 298 K is 4.6 in the 1 molal NaCl solution; this is greater than the value of 4.3 obtained with pure SPC/E water in our previous studies.<sup>34</sup> At 683 K, the coordination number of water in the 1 molal NaCl solution is about 4.1 for the SPC model. This is close to the value observed of 3.8 in simulations of pure SPC/E water<sup>22,23</sup> at the same temperature.

The extent of hydrogen bonding at higher temperatures is expected to be less. Figures 3 and 4 which show the oxygen–hydrogen  $g_{oh}(r)$  and hydrogen–hydrogen  $g_{hh}(r)$  radial distribution function at 298 K (0.997 g cm<sup>-3</sup>, dashed line) and at 683 K (0.35 g/cm<sup>3</sup>, solid line) in the 1 molal NaCl solution confirm this. The two peaks in  $g_{oh}(r)$  correspond to the two hydrogen atoms of a water molecule in the first shell and the first peak is usually referred to as the hydrogen bonding peak. As the temperature is increased, the height of this peak decreases signaling a breakdown of the hydrogen bonding network. Both peaks in Fig. 3 are also shifted away from the central oxygen at the higher tempera-

tures. The bimodal distribution in Fig. 4 becomes broader at high temperature with a shallower minimum between the maxima.

The peaks in these solvent distribution functions of a 1 molal sodium chloride solution are at the same locations as the corresponding peaks in pure water (not shown) for the same model, but the peak heights are again slightly different. These differences must represent slight perturbations of water structure by the sodium and chloride ions in a one molal sodium chloride solution.

## B. Solute–solvent atom distribution function

The solute–solvent atomic distribution functions for the 1 molal NaCl solutions at 298 K and 683 K are displayed in Figs. 5 and 6. The solvent densities at 298 K and 683 K are 0.997 g cm<sup>-3</sup> and 0.35 g cm<sup>-3</sup>, respectively. Figures 7 and 8 show the corresponding distribution functions for the 0.5 molal NaCl solutions at 683 K at solvent densities of 0.35

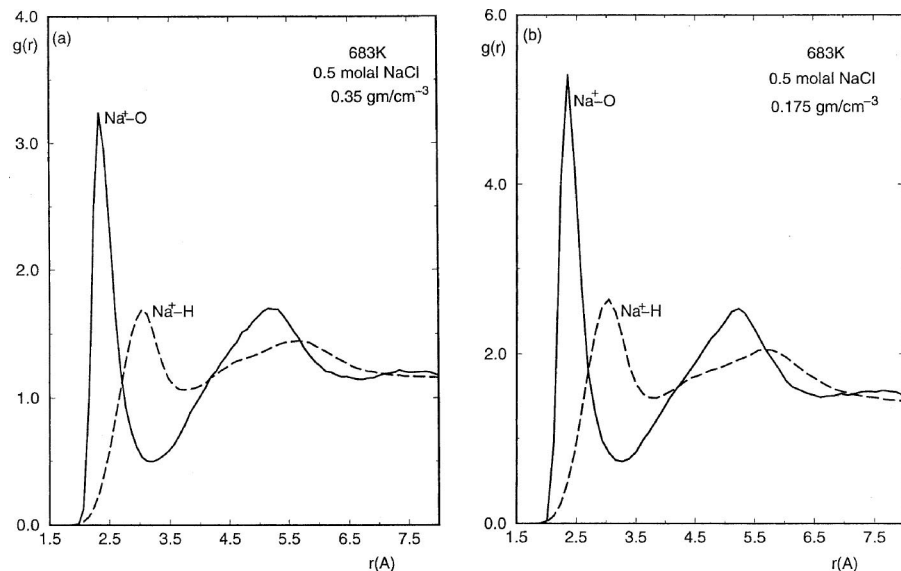


FIG. 7. Sodium–oxygen (solid line) and sodium–hydrogen (dashed line) radial distribution functions at 683 K (0.35 g cm<sup>-3</sup>, 0.175 g/cm<sup>-3</sup>) in a 0.5 molal NaCl solution in SPC water. The sodium–oxygen peaks are correlated with the corresponding sodium–hydrogen peaks. Corresponding results for one molal sodium chloride are in Fig. 5(b).

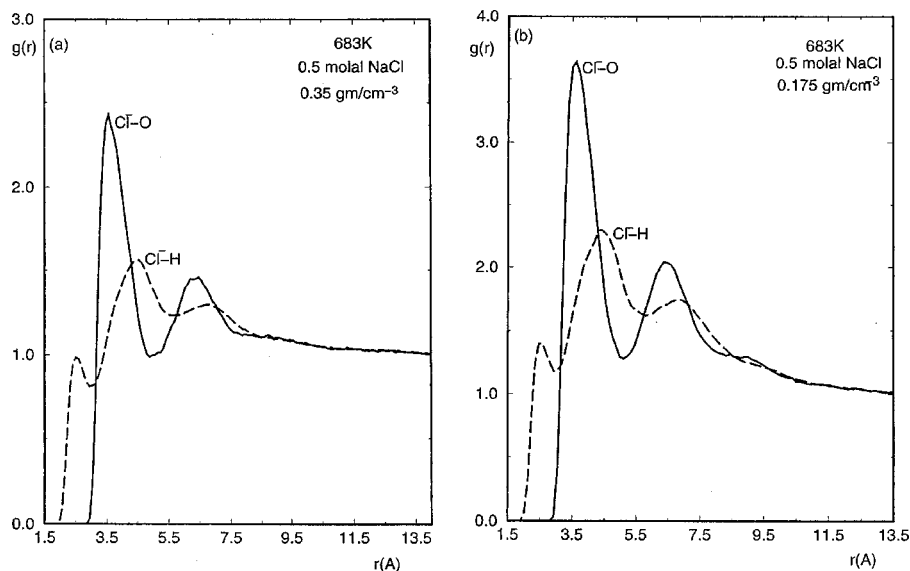


FIG. 8. Chloride–hydrogen (dashed line) and chloride–oxygen (solid line) radial distribution functions at 683 K ( $0.35 \text{ g/cm}^{-3}$ ,  $0.175 \text{ g/cm}^{-3}$ ) in a 0.5 molal NaCl solution in SPC water. The chloride–hydrogen peaks are correlated with the corresponding chloride–oxygen peaks. Corresponding results for one molal sodium chloride are in Fig. 6(b).

and  $0.175 \text{ g cm}^{-3}$ , respectively. The  $\text{Na}^+$  and  $\text{Cl}^-$  ion–solvent distribution functions in the 1 molal and 0.5 molal NaCl solutions at 683 K are significantly different from the functions for the infinitely dilute solutions that are discussed elsewhere<sup>22,23</sup> and reproduced in Figs. 5(c) and 5(d). In contrast to this, the ion–solvent distribution functions at infinite dilution (not shown) and in a 1 molal NaCl [Fig. 5(a)] solution remain essentially the same at 298 K. The implication is that sodium or chloride ions in NaCl solutions of finite concentration at 683 K are in a completely different environment from the corresponding solutions at infinite dilution. We will see that this is due to ion pairing and clustering of ions in concentrated solutions at elevated temperatures.

As pointed out earlier, the solvent distribution functions, at both temperatures (298 K and 683 K) are slightly perturbed by added electrolyte, in contrast to the solute–solvent distribution functions. Although the first Na–O and Cl–H peaks in the 683 K solution at infinite dilution are shifted only slightly from their positions at room temperature, the peak heights are different. The hydration numbers in the first

shells of the sodium and chloride ions are calculated from Eq. (9), with  $g_{oo}(r)$  replaced by  $g_{io}(r)$ , and  $R_U$  given by the position of the first minimum in this distribution function which changes with temperature and solvent density.<sup>24</sup> The hydration numbers of ions in the 1 molal NaCl solutions at 298 K displayed in Table II remain essentially the same as the numbers at infinite dilution. This is not so for the hydration numbers calculated at 683 K, which decrease progressively with electrolyte concentration.

Figure 5(b) shows three prominent peaks at 683 K in the sodium oxygen (Na–O) and sodium hydrogen (Na–H) radial distribution functions, with the peak of one correlated with a corresponding peak of the other that is in close proximity. The three peaks indicate the presence of three different environments for  $\text{Na}^+$  ions in 1 molal sodium chloride. Likewise, Fig. 6(b) shows the presence of three different environments for chloride atoms at 683 K, that are absent at 298 K. Similar peak correlations are observed in the ion–oxygen and ion–hydrogen distribution functions displayed in Figs. 7 and 8 for the sodium and chloride ions at 683 K in 0.5 molal

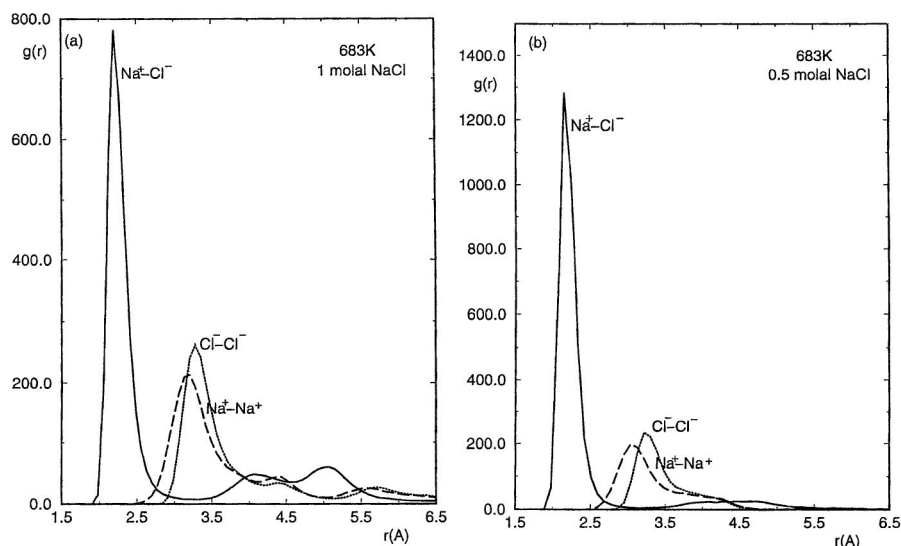


FIG. 9. Sodium–chloride (solid line), sodium–sodium (dashed line), and chloride–chloride (dotted line) radial distribution functions at 683 K in a 1 and 0.5 molal NaCl solution in SPC water. The sodium–chloride distribution function shows a strong peak at contact ion distance of 2.1 Å. Note the prominent peaks in the sodium–sodium and chloride–chloride distribution functions that suggest ion clustering in these systems.

sodium chloride solutions. We conclude that the immediate environment of the  $\text{Na}^+$  and the  $\text{Cl}^-$  ions in a sodium chloride solution of finite concentration (0.5 or one molal in concentration) at ambient conditions changes dramatically as the temperature is raised to 683 K. The reason for this is apparent from examining the ion–ion distribution functions of the sodium chloride solutions.

### C. Ion–ion distribution functions in sodium chloride solutions

Figure 9 displays the sodium chloride (solid line), sodium–sodium (dashed line), and chloride–chloride (dotted line) distribution functions at 683 K in SPC water in 1 molal and 0.5 molal solutions in which the solvent density is  $0.35 \text{ g cm}^{-3}$ . The sodium chloride distribution function shows three broad peaks in the 1 molal NaCl solution and two peaks (one broad and the other diffuse) in the 0.5 molal solution. The number of  $\text{Cl}^-$  ions paired with a sodium ion in the first, second, and third coordination shells are 3.5, 5.0, and 1.5 in the 1 molal NaCl solution, and 2.3 and 1.1 in the first and second coordination shells of the 0.5 molal solution, respectively. The Na–Na and Cl–Cl distribution functions also show peaks at nearly the same locations with small differences in the heights of the peaks. This indicates the presence of significant amount of clustering of positive and negative ions that goes beyond simple ion pairing. It is confirmed by snapshots of equilibrated configurations of the 1 molal and 0.5 molal solutions of sodium chloride shown in Fig. 10, where the sodium and chloride ions are seen to be obviously clustered together. In contrast to the single cluster found at 683 K in the 1 molal NaCl solution, equilibrium configurations of 0.5 molal solutions at solvent densities of  $0.35 \text{ g cm}^{-3}$  and  $0.175 \text{ g cm}^{-3}$  shows at least three clusters with varying amounts of  $\text{Na}^+$  and  $\text{Cl}^-$  ions.

Figure 11 displays the corresponding distribution functions and Fig. 12 a snapshot of an equilibrium configuration of the 1 molal NaCl solution at 298 K and solvent density of  $0.997 \text{ g cm}^{-3}$ . In this case, the sodium and chloride ions show no evidence of significant ion pairing. The sharp peak in the Na–Cl distribution function corresponds to the presence of a contact ion pair, but the number of pairs associated with this peak is only 0.1 showing that this is indeed very small. The second peak in this distribution function corresponds to the presence of a single solvent separated ion pair at equilibrium. Beyond this point, the Na–Cl distribution function reaches a plateau at large distances of separation between the ions. Our studies agree with Oelkers and Hegelson's<sup>32</sup> prediction of multiple ion association and cluster formation in supercritical aqueous electrolytes.

## IV. DIFFUSION COEFFICIENT

In this section we discuss the diffusion coefficients of the  $\text{Na}^+$  and  $\text{Cl}^-$  ions calculated from the velocity autocorrelation functions  $\langle \mathbf{v}(t) \cdot \mathbf{v}(0) \rangle$  using the relation

$$D = \frac{1}{3} \int_0^\infty \langle \mathbf{v}(t) \cdot \mathbf{v}(0) \rangle dt. \quad (10)$$

We compare the diffusion coefficients in Table III with the corresponding values for sodium and chloride ions at infinite dilution in water at 683 K and 298 K using the same model potentials.<sup>22,23,33–35</sup>

Table III indicates large increases in diffusion coefficients of sodium and chloride ions with temperature. The decrease in the diffusion coefficient with salt concentration is relatively greater at 683 K than at 298 K. The diffusion coefficients of the ions increase with decreasing solvent density as seen from the two sets of results for a 0.5 molal solution at 683 K.

The diffusion coefficients of  $\text{Na}^+$  and  $\text{Cl}^-$  ions in a 1 molal NaCl solution at 683 K are the same and smaller by a factor of 2 than the diffusion coefficients of the same ions at infinite dilution at 683 K. The average diffusion coefficients of the sodium and chloride ions in the 0.5 molal NaCl solutions at 683 K are also the same and smaller than the corresponding values at infinite dilution.

The equality of the diffusion coefficients of the sodium and chloride ions in the one molal solution is explained by the formation of a cluster of these ions which tends to move together as a whole, leading also to a lower diffusion coefficient. This is further supported by the similarity of the velocity autocorrelation functions of  $\text{Na}^+$  and  $\text{Cl}^-$  in 1 molal NaCl solution at 683 K shown in Fig. 13(a) in contrast to the corresponding functions for the single ions at infinite dilution at the same temperature depicted in Fig. 13(b). Note the significant differences between the two systems shown in Figs. 13(a) and 13(b). The decay in the velocity auto correlation functions at short times are also different in the two figures. The reason is that at infinite dilution the  $\text{Na}^+$  and the  $\text{Cl}^-$  ions are moving in the solvation shells of water molecules, while in the 1 molal sodium chloride the ions are oscillating in a cluster of  $\text{Na}^+$  and  $\text{Cl}^-$  ions that also contains water molecules. Figure 14 makes the same comparisons between the velocity autocorrelation functions of  $\text{Na}^+$  and  $\text{Cl}^-$  for the same systems (1 molal NaCl solution and infinitely dilute solutions) but at 298 K. In this case clustering is absent and the velocity autocorrelation functions of the two ions are very different in both the one molal and infinitely dilute solutions.

There is one caveat concerning the velocity autocorrelation functions of the ions in concentrated NaCl solutions depicted in Figs. 13 and 14 which are averages for each ion. The velocity auto correlation functions of the individual ions at 0.5 molal as displayed in Figs. 15(a) and 15(b) can be grouped into three categories indicating the presence of at least three different clusters, with varying amounts of  $\text{Na}^+$  and  $\text{Cl}^-$ . They correspond to the ions in three different ion clusters that are found in the 0.5 molal solution at a solvent density of  $0.35 \text{ g cm}^{-3}$  shown in Fig. 10. Similar conclusions apply to the solutions at the same molality (0.5 molal) but at a solvent density of  $0.175 \text{ g cm}^{-3}$ . In contrast to this we find only a single cluster in the one molal sodium chloride solution at 683 K in the discrete SPC solvent model for water.

## V. SIMULATIONS IN A CONTINUUM SOLVENT

To further understand the transformations that occur in the 1 molal sodium chloride solution with rise in tempera-



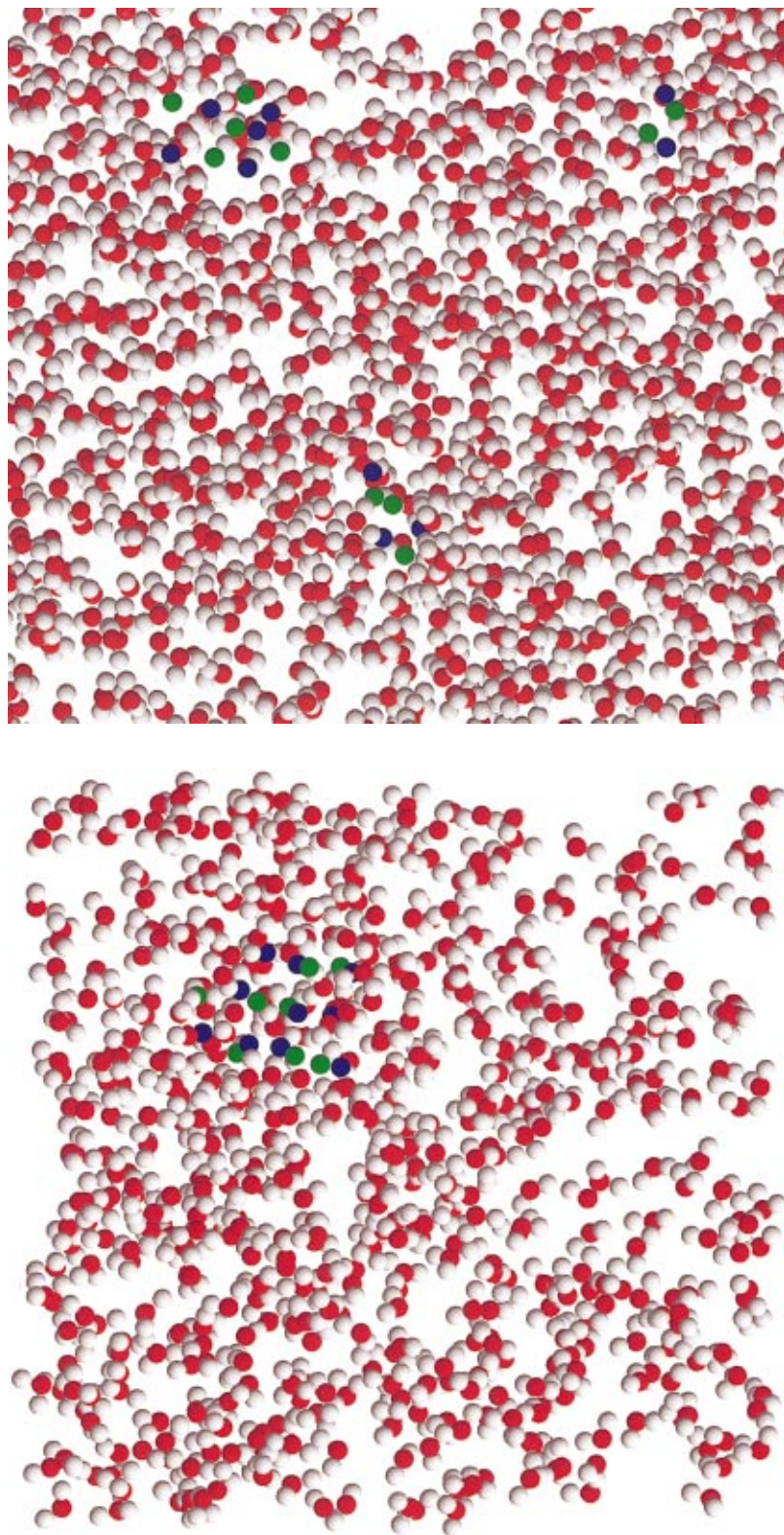


FIG. 10. (Color) Snapshots of 0.5 molal and 1 molal NaCl aqueous solutions in SPC water at 683 K. The oxygen and hydrogen atoms in water are represented as red and gray circles, respectively.  $\text{Na}^+$  ions are represented in blue, and  $\text{Cl}^-$  ions in green. Note the presence of a single NaCl cluster in the 1 molal NaCl solution (bottom figure) whereas in the 0.5 molal NaCl solution there are three different NaCl clusters (top figure). The solvent density is  $0.35 \text{ g cm}^{-3}$ .

ture, we removed the SPC water molecules in our system and replaced it with a continuum of dielectric constant  $\epsilon=78.0$  at room temperature and  $\epsilon=5.0$  at 683 K. The calculated  $\text{Na}^+\text{Na}^+$ ,  $\text{Cl}^-\text{Cl}^-$ , and  $\text{Na}^+\text{Cl}^-$  radial distribution functions at 298 K and 683 K are shown in Figs. 16 and 17.

At 298 K, the  $\text{Na}^+\text{Na}^+$  and  $\text{Cl}^-\text{Cl}^-$  radial distribution functions reach plateaus without any significant peaks. However, the NaCl distribution function shows a broad peak

around  $2.8 \text{ \AA}$  in contrast to the sharp peak at  $2.1 \text{ \AA}$  present for this system using a SPC model for water (see Fig. 11). The number of diatomic molecules corresponding to this peak is 0.1. When the temperature is increased, our simulation studies of the NaCl solutions with a continuum and molecular models of the solvent water lead to  $\text{Na}^+\text{Cl}^-$ ,  $\text{Na}^+\text{Na}^+$ , and  $\text{Cl}^-\text{Cl}^-$  distribution functions displaying many similar features, but there are important differences in detail.

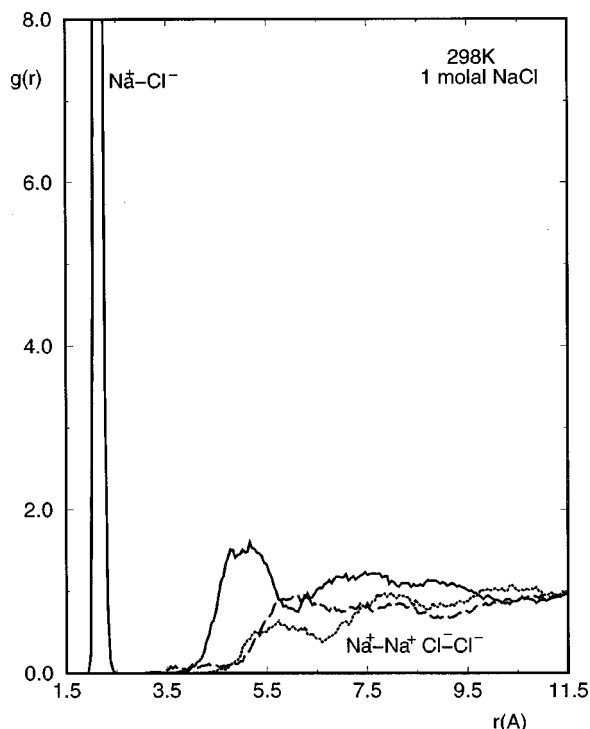


FIG. 11. Sodium–chloride (solid line), sodium–sodium (dashed line), and chloride–chloride (dotted line) radial distribution functions at 298 K in a 1 molal NaCl solution of SPC water. The sodium–chloride distribution function shows a narrow peak (peak height 38) at contact ion distance of 2.1 Å and a broad peak around 5 Å. The sodium–sodium and chloride–chloride distribution functions increase and reach a plateau.

At a supercritical temperature of 683 K, the molecular (Fig. 9) and continuum models (Fig. 17) of a 1 molal NaCl solution predict a strong peak in the NaCl distribution function at a distance between 2.1–2.4 Å. Also in both models, the Na–Na and Cl–Cl distribution functions have broader peaks at about the same locations between 3.2–4.5 Å. Taken collectively together, this indicates clustering of the sodium and chloride ions in the system.

The representation of the solvent by discrete charged models like the SPC or SPC/E models for water, shields the interactions between the ions  $\text{Na}^+$  and  $\text{Cl}^-$ . At room temperature, water molecules also tend to form hydrogen bonds with their neighbors further contributing to the shielding of the  $\text{Na}^+$  and  $\text{Cl}^-$  ions. This effect is represented by a large dielectric constant of 78 in the continuum treatment at ambient conditions. As the temperature is increased, the hydro-

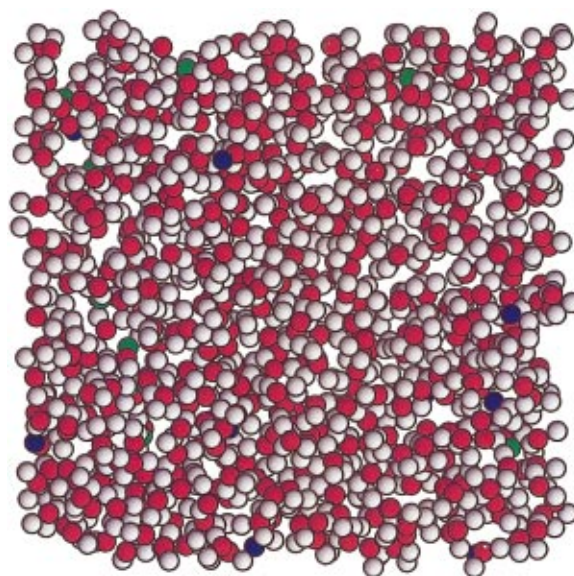


FIG. 12. (Color) A snapshot of the 1 molal NaCl system in SPC water at 298 K. Each  $\text{Na}^+$  and  $\text{Cl}^-$  ion is well solvated by water molecules.  $\text{Na}^+$  ions are represented by blue colored circles and the  $\text{Cl}^-$  ion by green colored circles. The solvent density is  $0.997 \text{ g cm}^{-3}$ .

gen bond network of water molecules breaks down, leading to significant attraction between the  $\text{Na}^+$  and  $\text{Cl}^-$  ions in the molecular treatment. In the continuum treatment this is represented by a smaller dielectric constant of 5, at 683 K. The basic trends in both molecular and continuum treatments, at the two temperatures (298 K and 683 K) are thus the same. At room temperature (298 K) sodium chloride solutions are fully dissociated and the  $\text{Na}^+$  and  $\text{Cl}^-$  ions are mostly separated from each other. This is evident from the fact that the Na–Na and Cl–Cl distribution functions in the molecular (Fig. 11) and continuum (Fig. 16) treatment reach plateaus without any prominent peaks in these functions.

## VI. DISCUSSION AND CONCLUSIONS

Our molecular dynamics simulations of sodium chloride solutions at 298 K and at 683 K using a discrete simple point charge models (SPC and SPC/E) for the solvent provide a detailed picture of the association of ions at high temperatures that goes beyond simple ion pairing. The solvent densities are  $0.997 \text{ g cm}^{-3}$  at 298 K, and 0.35 and  $0.175 \text{ g cm}^{-3}$  at 683 K. The concentrations of the sodium chloride solutions are 0.5 and 1 molal, and the results allow an informa-

TABLE III. Diffusion coefficients  $D(10^{-5} \text{ cm}^2 \text{ s}^{-1})$  of  $\text{Na}^+$  and  $\text{Cl}^-$  ions at 683 K and 298 K at infinite dilution and in 1 molal and 0.5 molal NaCl solutions at different solvent densities  $\rho_w(\text{g/cm}^3)$ .

Ion	Temp= $\rho_w(\text{g cm}^{-3})=0.35$	$D(10^{-5} \text{ cm}^2 \text{ s}^{-1})$			System
		683 K	0.175	298 K	
$\text{Na}^+$	$\infty$ diln	35	36	1.28	1 $\text{Na}^+$ , 215 SPC/E water
$\text{Cl}^-$	$\infty$ diln	34	44	1.77	1 $\text{Cl}^-$ , 215 SPC/E water
$\text{Na}^+$	1 M	17		1.18	10 $\text{Na}^+$ , 10 $\text{Cl}^-$ , 555 SPC water
$\text{Cl}^-$	1 M	17		1.48	10 $\text{Na}^+$ , 10 $\text{Cl}^-$ , 555 SPC water
$\text{Na}^+$	0.5 M	24	29		10 $\text{Na}^+$ , 10 $\text{Cl}^-$ , 1110 SPC water
$\text{Cl}^-$	0.5 M	24	29		10 $\text{Na}^+$ , 10 $\text{Cl}^-$ , 1110 SPC water

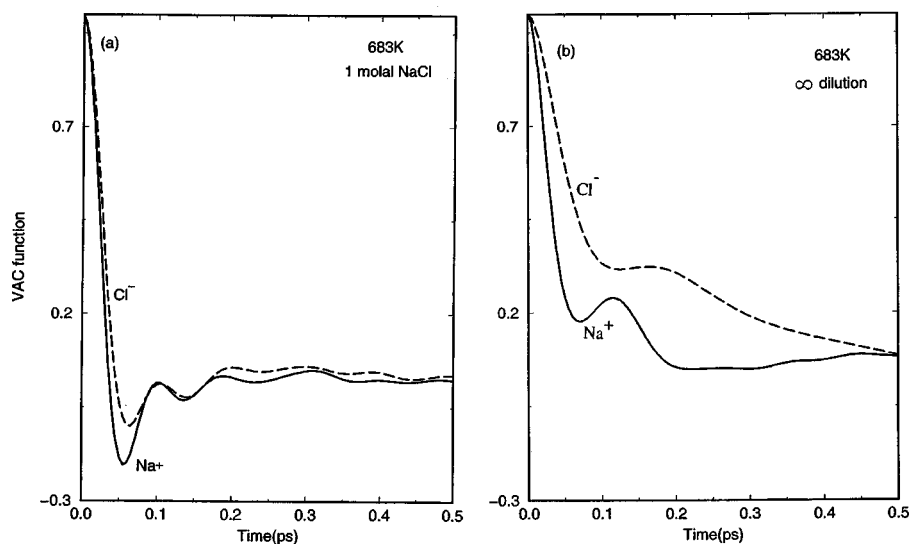


FIG. 13. Velocity auto correlation function of  $\text{Na}^+$  and  $\text{Cl}^-$  ions in the one molal NaCl solution at 683 K in SPC water at a solvent density of  $0.35 \text{ g cm}^{-3}$ . The oscillations at short time for both ions are nearly in phase. (b) The same function for  $\text{Na}^+$  and  $\text{Cl}^-$  at infinite dilution in SPC/E water at 683 K at a solvent density of  $0.35 \text{ g cm}^{-3}$ . There are significant differences in the phases of the oscillations of this function for the two ions.

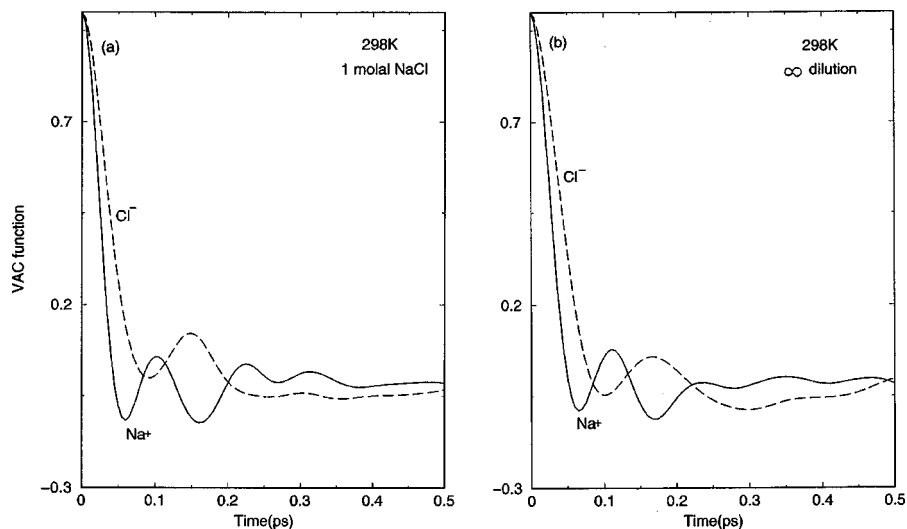


FIG. 14. Velocity autocorrelation function of  $\text{Na}^+$  and  $\text{Cl}^-$  ions in (a) a 1 molal NaCl solution at 298 K in SPC water and (b) at infinite dilution, both in SPC/E water at a density of  $0.997 \text{ g cm}^{-3}$  at 298 K.

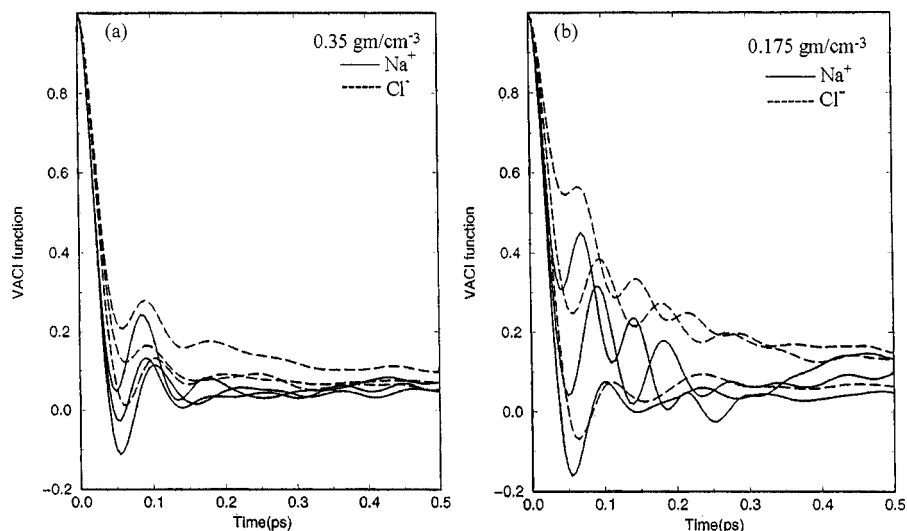


FIG. 15. Velocity autocorrelation functions of  $\text{Na}^+$  and  $\text{Cl}^-$  ions in three different ion clusters observed in a 0.5 molal NaCl solution in SPC water at 683 K and solvent densities of (a)  $0.35 \text{ g/cm}^{-3}$  and (b)  $0.175 \text{ g/cm}^{-3}$ .



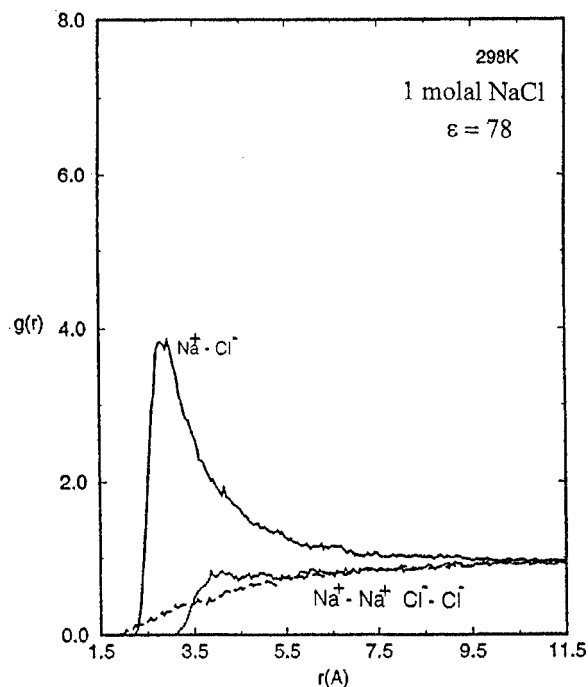


FIG. 16. Sodium–chloride (solid line), sodium–sodium (dashed line), and chloride–chloride (dotted line) distribution functions in a 1 molal sodium chloride solution at 298 K, with a continuum treatment of the solvent with an effective dielectric constant of 78. Figure 11 shows the corresponding results for SPC water at a solvent density of  $0.997 \text{ g/cm}^{-3}$ .

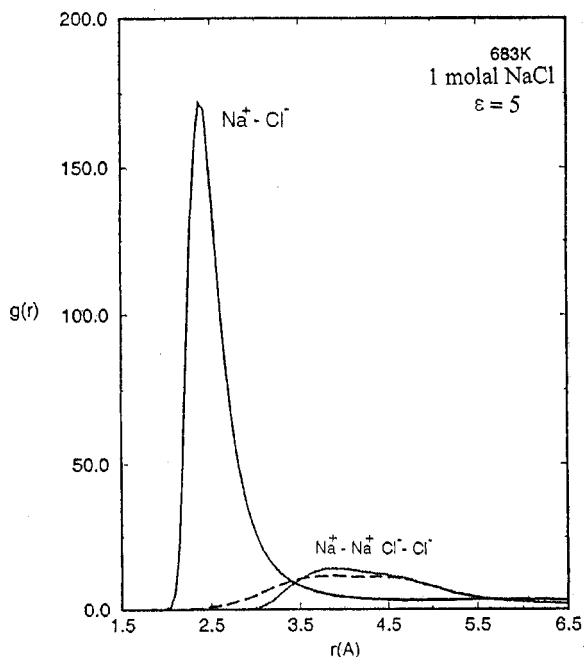


FIG. 17. Sodium–chloride (solid line), sodium–sodium (dashed line), and chloride–chloride (dotted line) distribution functions in a 1 molal sodium chloride solution at 683 K in which the solvent is treated as a continuum with a dielectric constant of 5. Figure 9(a) shows the corresponding results for 1 molal sodium chloride in SPC water at a solvent density of  $0.35 \text{ g/cm}^{-3}$ . The strong peak at contact in the  $\text{Na}^+ - \text{Cl}^-$  distribution functions occur at the same distance in both figures, but the peak heights and other details of the structure differ. The  $\text{Na}-\text{Na}$  and  $\text{Cl}-\text{Cl}$  radial distribution functions show peaks at approximately the same locations for both solvent models but the peaks are less prominent in the continuum model.

tive comparison with the properties of sodium and chloride ions in aqueous solutions at infinite dilution. Comparisons are also made with simulations of one molal sodium chloride at 683 K and 298 K, using continuum solvent models with dielectric constants of 5 and 78, respectively.

We find similar qualitative behavior of the solute pair distribution functions in our simulations of sodium and chloride ions in concentrated solutions at ambient temperatures using both discrete and continuum molecular solvent. However, at supercritical temperatures, there is significant difference between these systems. The simulations of 0.5 and 1 molal sodium chloride solutions in SPC water show  $\text{Na}^+$  and  $\text{Cl}^-$  ions clustering together with water molecules participating in cluster formation. The ions in our simulation of a 1 molal solution of sodium chloride formation a single large cluster of ten sodium and ten chloride ions equal to the total number of ions in our system which tend to diffuse as a single entity. This may correspond to a supersaturated solution. After a 200 ps production run, snapshots of the 0.5 molal NaCl solutions at two different solvent densities 683 K reveal the presence of three ion clusters of different size solvated by water molecules. This picture is supported by calculations of the individual velocity autocorrelation functions of the ions.

At both temperatures (298 K and 683 K), the ion distribution functions of continuum and molecular solvent models of ionic solutions have peaks at nearly the same locations. However, the peak heights in the two models of the same electrolyte solution are different, and the amount of the ion pairing in the molecular treatment is always greater than that of the continuum treatment. This suggests that the solvent molecules also participate in cluster formation and continuum models oversimplify the nature of pairing and clustering in ionic solutions especially at supercritical temperatures.

We have observed that the peak heights in these distribution functions at 683 K changed back and forth with the simulation time but the ion solvent distribution functions  $\text{NaO}$ ,  $\text{ClO}$ ,  $\text{NaH}$ ,  $\text{ClH}$ , etc. are very stable. This could be a manifestation of the break down and reformation of clusters that occur during the time scale of our simulations which is about 200 ps and the small number of ions in our simulations. In order to get better averages of the ion–ion distribution functions, it would be necessary to perform simulations for at least a several nanoseconds using a larger system. However, this may add only little new information to what we already have, since the fluctuations in the ion–ion distribution functions over shorter time scales would still remain. All of the ion–solvent distribution functions at 683 K on the other hand were stable and reproducible in shorter 200 ps runs.

Our studies are in accord with molecular dynamics simulations of Driesner *et al.*<sup>24</sup> and Tester *et al.*<sup>25,26</sup> of the equilibrium properties of  $\text{Na}^+$  and  $\text{Cl}^-$  ions in aqueous solutions, which also suggested ion pairs, triplets and larger charged and uncharged clusters of varying size in NaCl solutions at supercritical temperatures. We have complemented this by investigating the diffusion coefficients of ions in concentrated solutions of sodium chloride using discrete point



charge models for the solvent and by studying the behavior of these solutions when the solvent is treated as a continuum dielectric. Our simulations lend support to Oelkers and Helgeson's<sup>32</sup> predictions of multiple ion association and cluster formation in supercritical aqueous electrolyte solutions. These predictions are based on experimental evidence<sup>1,36,37</sup> and free energy minimization of an association model of ions in a structureless low dielectric medium.<sup>32</sup> A detailed molecular theory that explains the structure and dynamics of these solutions including cluster formation has yet to be developed.

## ACKNOWLEDGMENT

This study was supported by Grant No. CHE-9961336 from the National Science Foundation.

- <sup>1</sup>(a) A. S. Quist and W. L. Marshall, *J. Phys. Chem.* **72**, 684 (1968); **72**, 1545 (1968); (b) L. A. Dunn and W. L. Marshall, *ibid.* **73**, 723 (1969); (c) J. D. Frantz and W. L. Marshall, *Am. J. Sci.* **282**, 1666 (1982).
- <sup>2</sup>R. H. Wood, M. S. Gruskiewicz, and G. H. Zimmerman, *J. Phys. Chem.* **99**, 11612 (1995).
- <sup>3</sup>D. P. Fernandez, A. R. H. Goodwin, E. W. Lemmon, J. M. H. Levelt Sengers, and R. C. Williams, *J. Phys. Chem. Ref. Data* **26**, 1125 (1997).
- <sup>4</sup>(a) R. D. Mountain and A. Wallquist "Collection of Results for SPC/E water," NIST Report No. 5778, 1996; (b) A. Wallquist and R. Mountain, *Rev. Comput. Chem.* **13**, 183 (1999).
- <sup>5</sup>S. T. Cui and J. G. Harris, *J. Phys. Chem.* **99**, 2900 (1995).
- <sup>6</sup>M. Neumann, in *Physical Chemistry of Aqueous Solutions*, edited by H. J. White Jr., J. V. Sengers, D. V. Neumann, and J. C. Bellows (Begell House, New York, 1995).
- <sup>7</sup>(a) Y. Guissiani and B. Guillot, *J. Chem. Phys.* **99**, 3049 (1993); (b) B. Guillot and Y. Guissiani, *ibid.* **98**, 728 (1994).
- <sup>8</sup>H. L. Friedman, *A Course in Statistical Mechanics* (Prentice-Hall, Englewood Cliffs, 1985).
- <sup>9</sup>(a) H. Luo and S. Tucker, *Theor. Chem. Acc.* **96**, 84 (1997); (b) S. Tucker and M. W. Maddox, *J. Phys. Chem. B* **102**, 2537 (1998).
- <sup>10</sup>(a) P. J. Rossky and K. P. Johnston, "Chemistry in supercritical water: Insights from theory and simulation," in Proceedings of the International Conference on the Properties of Water and Steam, Toronto, 1999; (b) G. E. Bennet, P. J. Rossky, and K. P. Johnston, *J. Phys. Chem.* **99**, 16136 (1995); (c) L. W. Flanagan, P. B. Balbuena, K. P. Johnston, and P. J. Rossky, *ibid.* **99**, 5196 (1995); (d) P. B. Balbuena, K. P. Johnston, P. J. Rossky, and J.-K. Lee, *J. Phys. Chem. B* **102**, 3806 (1998).
- <sup>11</sup>(a) A. A. Chialvo, P. T. Cummings, H. D. Cochran, J. M. Simonson, and R. E. Mesmer, *J. Chem. Phys.* **103**, 9379 (1995), and references therein.
- <sup>12</sup>(a) L. X. Dang and B. M. Pettitt, *J. Phys. Chem.* **94**, 4303 (1990); (b) D. E. Smith and L. X. Dang, *J. Chem. Phys.* **100**, 3757 (1994).
- <sup>13</sup>(a) R. Rey and E. Guardia, *J. Phys. Chem.* **96**, 4712 (1992); (b) E. Guardia, R. Rey, and J. A. Padro, *Chem. Phys.* **155**, 187 (1991); (c) R. Rey, E. Guardia, and J. A. Padro, *J. Chem. Phys.* **97**, 1343 (1992).
- <sup>14</sup>(a) M. Berkowitz, A. Kairim, J. A. McCammon, and P. J. Rossky, *Chem. Phys. Lett.* **105**, 577 (1984); (b) A. C. Belch, M. Berkowitz, and J. A. McCammon, *J. Am. Chem. Soc.* **108**, 1755 (1986); (c) O. A. Karim and J. A. McCammon, *ibid.* **108**, 1762 (1986); (d) O. A. Karim and J. A. McCammon, *Chem. Phys. Lett.* **132**, 219 (1986); (e) J. A. McCammon, O. A. Karim, T. P. Lybrand, and C. F. Wong, *Ann. N.Y. Acad. Sci.* **482**, 210 (1986).
- <sup>15</sup>P. L. Geissler, G. Dellago, and D. Chandler, *J. Phys. Chem.* **103**, 3706 (1999).
- <sup>16</sup>(a) M. Fisher, *J. Stat. Phys.* **75**, 1 (1994); (b) *J. Phys.: Condens. Matter* **8**, 9103 (1996).
- <sup>17</sup>G. Stell, *J. Stat. Phys.* **78**, 197 (1995).
- <sup>18</sup>J. M. H. Levelt Sengers and J. A. Given, *Mol. Phys.* **80**, 899 (1993).
- <sup>19</sup>M. A. Anisimov and J. V. Sengers, "Crossover critical phenomena in aqueous solutions," in Proceedings of the 13th International Conference on the Properties of Water and Steam, Toronto, Canada, September, 1999.
- <sup>20</sup>V. M. Nabutovskii, N. A. Memov, and Yu. G. Peisakovich, *Sov. Phys. JETP* **51**, 1111 (1980).
- <sup>21</sup>J. S. Høye and G. Stell, *J. Phys. Chem.* **94**, 7899 (1990).
- <sup>22</sup>J. C. Rasaiah, J. P. Noworyta, and S. Koneshan, *J. Am. Chem. Soc.* (submitted).
- <sup>23</sup>J. P. Noworyta, S. Koneshan, and J. C. Rasaiah, *J. Am. Chem. Soc.* (submitted).
- <sup>24</sup>T. Driesner, T. M. Steward, and I. G. Tironi, *Geochim. Cosmochim. Acta* **62**, 3096 (1998).
- <sup>25</sup>J. W. Tester, P. A. Marrone, M. M. DiPippo, K. Sako, M. T. Reagan, T. Arias, and W. A. Peters, *J. Supercrit. Fluids* **13**, 225 (1998).
- <sup>26</sup>M. T. Reagan, J. G. Harris, and J. W. Tester, *J. Phys. Chem. B* **103**, 7936 (1999).
- <sup>27</sup>(a) G. Hummer, D. M. Soumpasis, and M. Neumann, *J. Phys.: Condens. Matter* **6**, A141 (1994); (b) *Mol. Phys.* **81**, 115 (1994).
- <sup>28</sup>J. V. Sengers and J. M. H. Levelt-Sengers, *Annu. Rev. Phys. Chem.* **37**, 189 (1986).
- <sup>29</sup>B. M. Pettit and P. J. Rossky, *J. Chem. Phys.* **84**, 5836 (1986).
- <sup>30</sup>M. L. Huggins and J. E. Mayer, *J. Chem. Phys.* **1**, 509 (1933).
- <sup>31</sup>(a) L. X. Dang, *Chem. Phys. Lett.* **200**, 21 (1992); (b) L. X. Dang and B. C. Garrett, *J. Chem. Phys.* **99**, 2972 (1993); (c) L. X. Dang and P. Kollmann, *J. Phys. Chem.* **99**, 55 (1995); (d) L. X. Dang, *J. Am. Chem. Soc.* **117**, 6954 (1995); (e) L. X. Dang, *J. Chem. Phys.* **102**, 3483 (1995).
- <sup>32</sup>E. H. Oelkers and H. C. Helgeson, *Science* **261**, 888 (1993b), and references therein.
- <sup>33</sup>S. H. Lee and J. C. Rasaiah, *J. Phys. Chem.* **100**, 1420 (1996).
- <sup>34</sup>S. Koneshan, J. C. Rasaiah, R. M. Lynden-Bell, and S. H. Lee, *J. Phys. Chem.* **102**, 4193 (1998).
- <sup>35</sup>S. Koneshan, J. C. Rasaiah, and R. M. Lynden-Bell, *J. Am. Chem. Soc.* **120**, 12041 (1998).
- <sup>36</sup>E. U. Franck, *Phys. Chem.* **8**, 92 (1956).
- <sup>37</sup>G. Ritzert and E. U. Franck, *Ber. Bunsenges. Phys. Chem.* **72**, 798 (1968).